

The $3^2S_{1/2}$ - $3^2D_{5/2}$ interval in atomic hydrogen. I. Two-photon line-shape theory

D. A. Van Baak, B. O. Clark,* and F. M. Pipkin

Lyman Laboratory of Physics, Harvard University, Cambridge, Massachusetts 02138

(Received 8 August 1978)

This paper reports a theoretical treatment of the line shape for two-photon transitions. The time-dependent perturbation-theory treatment is equally appropriate for a fast atomic beam interacting with a microwave field in a waveguide, and for laser excitation of a thermal beam. Two important features of the physical systems are successfully incorporated into the theory. First, the amplitude of the external field to which the atoms are exposed varies in time; the envelope function affects the resonance linewidth and power shift. Second, the theory includes the natural decay of the atomic states; the decay amplitude produces a novel "lifetime shift," which displaces the two-photon resonance from its expected location, even in the limit of weak external fields. This paper gives detailed predictions for shifts and other distortions caused by nonidealities of the experimental apparatus used for the measurement of the $3^2S_{1/2}$ - $3^2D_{5/2}$ transition in atomic hydrogen.

I. INTRODUCTION

The study of radio-frequency transitions among the fine-structure levels of hydrogen, begun with thermal hydrogen beams by Lamb and co-workers three decades ago, entered a new domain with the introduction of the fast-atomic-beam method.¹ The fast-atomic-beam technique made it possible to make beam measurements on atoms in the higher excited states and to use Ramsey's separated oscillatory field technique to obtain resonance lines whose widths are less than the natural linewidths. The recently reported measurements of the Lamb shift in the $n=2$ state of hydrogen demonstrate the power of this technique.^{2,3}

This paper and the succeeding paper report a second method that uses multiple-quantum transitions for improved measurements of the fine-structure intervals in atomic hydrogen which is made possible through the use of fast atomic beams.⁴ This technique has been used to measure the $2^2S_{1/2}$ - $2^2D_{5/2}$ fine-structure interval in the $n=3$ state of atomic hydrogen through a two-photon transition. This paper reports the theoretical treatment of the line shape; the succeeding paper reports the details of the measurement of this transition.

The motivation for the multiple-quantum technique came from the empirical observation that the precision of a spectroscopy experiment tends ultimately to be limited to some fraction of the experimental linewidth, and this limit is due as much to systematic errors as to statistical errors. The separated oscillatory fields technique reduces the linewidth at the cost of signal size; the multiple-quantum technique makes available transitions with a smaller natural linewidth.

As an example, consider the fine structure of the $n=3$ level of hydrogen. The conventional $3^2S_{1/2}$ -

$3^2P_{1/2}$ Lamb-shift resonance has a natural linewidth of 30 MHz, which is determined by the 5.4-nsec lifetime of the $3P$ state. By contrast, the $3^2S_{1/2}$ - $3^2D_{5/2}$ double-quantum resonance has a linewidth of 10 MHz, since the $3D$ state has a lifetime 3 times longer than that of the $3P$ state. Since both resonances indirectly measure the energy of the $3S$ state (which contains most of the radiative corrections), an improvement in accuracy by a factor of 3 would be expected for the double-quantum measurement over the conventional Lamb-shift transition.

Before the promise of this approach can be realized, however, two obstacles must be overcome. One must first arrange to observe a multiple-quantum transition under conditions of good signal-to-noise ratio and in a "clean," well-understood environment. The experiment by which this goal was attained is outlined in Sec. II of this paper, and described in detail in the following paper. The second requirement is a sufficiently detailed theoretical understanding of the multiple-quantum line shape such that the line can be "split" to a small fraction of its width. This is the subject of this paper. The results of this analysis are combined with the experimental data in the concluding sections of the following paper, where the result for the $3^2S_{1/2}$ - $3^2D_{5/2}$ interval is presented.

In addition to its immediate usefulness in reducing the data of the following paper, the theoretical results of this paper have general applicability to multiphoton experiments. The formalism used is especially suited to beam experiments wherein state preparation, interrogation, and detection are resolved in time, and it can be applied to laser as well as microwave transitions.

Before embarking on the calculations, it is instructive to compare these techniques with other theoretical approaches to multiphoton transitions.

For a Hamiltonian periodic in time, one can apply the techniques of Shirley⁵ to multiple-quantum transitions. In this approach, the $3^2S_{1/2}$ - $3^2D_{5/2}$ transition may be viewed as a level crossing, as the microwave frequency is varied, between the atom-field product states of $3S$ plus one photon and $3D$ minus one photon. Salwen⁶ has developed a useful variation of time-independent perturbation theory which reduces the multiple-quantum transition to an effective two-level problem. When combined with Shirley's techniques, many of the features of multiple-quantum transitions, such as the power shift, emerge in a simple manner. We have not used these techniques, however, in analyzing this experiment. The reason is that the Hamiltonian is not purely periodic, since the amplitude of the oscillating microwave field is itself varying in time. This envelope function has distinct and nontrivial consequences, and cannot be handled by these theoretical treatments. Our formalism is well suited to handle general envelope functions, such as the Gaussian envelope characteristic of laser fields.

A second feature of the atomic system for which the theory must account is the spontaneous decay of the atomic states. We have incorporated this by using the Bethe-Lamb prescription; this gives a non-Hermitian Hamiltonian and a nonunitary evolution operator.

The contents of this paper are as follows: Section II presents a simplified picture of the experiment in order to specify the requirements of the theory; Sec. III outlines the general formalism; Sec. IV introduces the time-dependent perturbation theory (TDPT) used for computation. In Sec. V we present the effective potential approximation, which greatly simplifies the calculation of multiple-quantum processes. We discuss in Secs. VI and VII the lifetime shift and power shift for the two-photon resonance. In Sec. VIII, the saturation behavior of the two-photon resonance is considered, and in Sec. IX we consider the small corrections required by nonidealities in the experimental situation. Section X summarizes our findings with a view toward analysis of the $3^2S_{1/2}$ - $3^2D_{5/2}$ transition in atomic hydrogen.

II. REQUIREMENTS FOR THE THEORY

One of the goals of this paper is to provide the theoretical machinery necessary to analyze and understand the fast-beam measurements of the $3^2S_{1/2}$ - $3^2D_{5/2}$ transition. Consequently we review here those features of the experimental apparatus which are relevant to the theory. The apparatus is outlined schematically in Fig. 1.

The study of the $3^2S_{1/2}$ - $3^2D_{5/2}$ transition starts



FIG. 1. Schematic diagram of the experimental apparatus used to investigate two-photon transitions.

in the region labeled "production," where a beam of atoms in the $3S$ state is formed by charge-exchange collisions with a fast ion beam. In the "interrogation" region, the atoms in the $3S$ state pass through a waveguide, which conducts microwaves perpendicular to the direction of the atomic beam, and undergo the two-photon transitions of interest. Subsequently, the beam passes through a "selection" region, which, through transitions to the $3P$ state, eliminates atoms in the $F=1$ hyperfine level of the $3S$ state, but which has little effect on the atoms in the $F=0$ state. Finally, in the "detection" region a photomultiplier monitors the $3^2S_{1/2}(F=0)$ population by the detection of Balmer α photons emitted in the spontaneous decay of $3S$ states. The $3P$ and $3D$ states formed in the charge-exchange process decay before they can travel to the photomultiplier tube, so that the photomultiplier signal is due primarily to the $3^2S_{1/2}(F=0)$ states. Thus what is needed is a detailed theory of the probability for atoms in $3^2S_{1/2}(F=0)$ states to pass through the waveguide region.

To a good approximation, the waveguide can be characterized as a region of electric field,

$$\vec{E}(t) = \hat{z}E \sin(\pi t/T) \cos(\omega t + \delta), \quad (1)$$

where an individual atom is inside the waveguide for $0 < t < T$. Refinements having to do with magnetic fields, stray polarizations of the microwave field, etc., are discussed in Sec. IX. Since the atomic beam is nearly monoenergetic, the use of a single transit time T for all the atoms is justified. However, atoms enter the waveguide at random times, so the transmission probabilities must eventually be averaged over δ , the phase of the field when the atom enters.

We expect a resonant decrease in the $3^2S_{1/2}(F=0)$ transmission probability as ω is scanned through the region

$$2\hbar\omega = E(3^2D_{5/2}(F=2)) - E(3^2S_{1/2}(F=0)). \quad (2)$$

The center of the resonance is located by sampling the signal at six points on the resonance line shape, which are symmetrically spaced about the center of the resonance.

Hereafter we use units in which $\hbar=1$, but leave \hbar 's in place on occasion for mnemonic purposes. We also choose for quantization axis the \hat{z} direction, the direction of polarization of the electric field in the waveguide.

III. THEORETICAL FORMALISM

To calculate the transmission probability for a hydrogen atom in the $3^2S_{1/2}(F=0)$ state to pass through the region of electric field described by Eq. (1), we need the matrix elements of the evolution operator corresponding to the Hamiltonian

$$\mathcal{H} = \mathcal{H}_0 - e\vec{E}(t) \cdot \vec{r}, \quad (3)$$

where \mathcal{H}_0 denotes the Hamiltonian of the field-free atom, and $-e\vec{E}(t) \cdot \vec{r}$ represents the interaction of the atomic dipole moment $-e\vec{r}$ with the external electric field. The use of this form of interaction, rather than the more familiar $-e\vec{A} \cdot \vec{p}$ term, has been fully justified in the literature.^{7,8} Even the effects of the diamagnetic $\vec{A} \cdot \vec{A}$ term are included (in higher order) in the $-e\vec{E} \cdot \vec{r}$ interaction. The use of a classical, rather than a quantized, form for the electric field $\vec{E}(t)$ has been considered elsewhere,⁹ and is justified basically because of the large photon number density of the microwave field. The effects of the magnetic dipole interaction are considered in Sec. IX.

With these assumptions about the form of the electric field and the interaction, only $\Delta m_F = 0$ transitions are induced, and the only states connected to the $3^2S_{1/2}(F=0)$ state by \mathcal{H} are those listed in Table I. There we also assign mnemonic labels to the states. Table II lists the matrix elements of z among these states, and Fig. 2 shows their values in an energy-level diagram. The diagram shows that the S state is connected to the D state by a two-photon transition via the intermediate P state. The S state will be power shifted by its coupling to the P and P' states, and similarly the D state by its coupling to the P state. The D' state is only peripherally involved.

TABLE II. Matrix elements of z (in units of a_0) among the states.

Matrix element	Value		Value squared
	Analytic	Numerical	
$\langle S z P \rangle$	6	6.000	36.00
$\langle P z D \rangle$	$\frac{9}{10}(30)^{1/2}$	4.930	24.30
$\langle S z P' \rangle$	$-3(2)^{1/2}$	-4.423	18.00
$\langle P' z D' \rangle$	$\frac{3}{2}(10)^{1/2}$	4.743	22.50
$\langle P z D' \rangle$	$-\frac{3}{10}(5)^{1/2}$	-0.671	0.45

The calculation of transition probabilities, line centers, etc., requires input values for the energies of the states in question. We adopt for these purposes Erickson's calculations¹⁰ of the $n=3$ energy levels (hyperfine structure neglected), with uncertainties on the order of a few kHz. The object of the experiment is to measure the S - D interval; the exact values adopted for the positions of the rest of the energy levels are not critical. We have calculated the hyperfine energies by the methods of Brodsky and Parsons,¹¹ again to 1-kHz accuracy, taking the precaution of including the Breit correction for the $3S$ state,^{12,13} and the effects of terms off diagonal in J in the $3P$ and $3D$ hyperfine structure.

The spontaneous decay of the atomic states is accounted for via the Bethe-Lamb prescription, which assigns to a level N the complex energy $E_N = \omega_N - \frac{1}{2}i\Gamma_N$, where ω_N is the Bohr frequency and Γ_N the decay rate. The validity of this approximation has been studied for hydrogen¹⁴; it introduces no appreciable error, chiefly because

TABLE I. Energy levels involved in the $3^2S_{1/2} \rightarrow 3^2D_{5/2}$ two-photon transition in the $n=3$ state of hydrogen. In the third column labeled Energy, the location of the $3^2S_{1/2}$ state with the assumption there is no hyperfine splitting is taken as the origin and none of the hyperfine splittings for the other states have been included; column 4 gives the hyperfine energies that must be added to column 3 to obtain the energy levels when the hyperfine structure is included. Column 5 gives the energy of the states when the hyperfine structure is included with the location of the $3^2S_{1/2}(F=0)$ state as origin.

State	Mnemonic	Energy (MHz)	hfs (MHz)	ω (10^9 sec^{-1})	Γ (10^9 sec^{-1})
$3^2S_{1/2}(F=0)$	S	0.0	-39.457	0.0	0.0063
$3^2P_{3/2}(F=1)$	P	2935.191	- 4.380	18.66274	0.1897
$3^2P_{1/2}(F=1)$	P'	- 314.898	+ 4.382	- 1.70311	0.1897
$3^2D_{5/2}(F=2)$	D	4013.197	- 1.577	25.45367	0.0647
$3^2D_{3/2}(F=2)$	D'	2929.859	+ 1.577	18.66668	0.0647

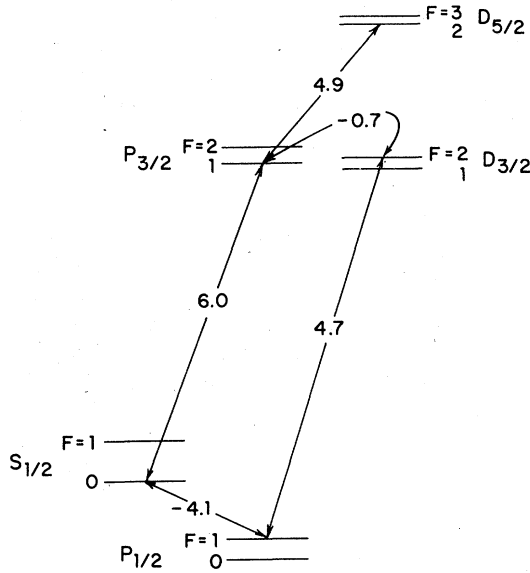


FIG. 2. Schematic level diagram for the $n=3$ states of atomic hydrogen (not to scale), showing allowed electric dipole transitions connected to the $3^2S_{1/2}$ ($F=0$) state by an electric field parallel to the z axis.

the separation of the states in question is very small compared to the optical energies released in their decays. (Whether the same assumption can be made in considering laser-driven transitions among decaying states requires further study.) The values of Γ_N appropriate to the states involved are included in Table I. They are calculated ignoring radiative and relativistic corrections, which should be much less than 1%. Any additional collision-induced decay of the states is also negligible, for background pressures typical of the experiment. The complex energy levels produced by the Bethe-Lamb prescription are taken to be the diagonal matrix elements of \mathcal{H}_0 .

The total Hamiltonian describes the time evolution of a five-state Hilbert space. We define the diagonal matrix element for the S state of this evolution operator to be $A(\omega, E, \delta)$. Since this represents the amplitude for transmission of the S state through the interaction region, the experimentally observed transmission probability is

$$P(\omega, E) = (2\pi)^{-1} \int_0^{2\pi} d\delta |A(\omega, E, \delta)|^2. \quad (4)$$

We define the signal to be the fractional decrease of this probability upon turning on the microwave field:

$$S(\omega, E) = [P(\omega, 0) - P(\omega, E)]/P(\omega, 0) \quad (5)$$

IV. TDPT EXPANSION

For reasons delineated in the introduction, we make a TDPT expansion of the S to S amplitude A in powers of E , the peak electric field, defining

$$A = \sum_{n=0}^{\infty} A^{(n)}, \quad (6)$$

where $A^{(n)}$ is of order E^n . It is easily seen that only terms of even n appear. It can be shown that this series converges; the series is useful because for moderate values of the electric field the low-order terms are dominant. Since the Hamiltonian is periodic in δ , the amplitude A and its TDPT expansion coefficients $A^{(n)}$ must be expressible as Fourier series in δ . The highest frequency component present in $A^{(n)}$ is $e^{\pm in\delta}$, so we can write

$$A = \sum_{n=0}^{\infty} \sum_{k=-n}^n A_k^{(n)} e^{ik\delta}. \quad (7)$$

With this expansion, the signal $S(\omega, E)$ defined by Eq. (5) can be calculated. After averaging over δ , we obtain

$$S(\omega, E) = -|A_0^{(0)}|^{-2} \left(2 \operatorname{Re}(A_0^{(0)*} A_0^{(2)}) + 2 \operatorname{Re}(A_0^{(0)*} A_0^{(4)}) \right. \\ \left. + \sum_{k=-2}^2 |A_k^{(2)}|^2 + 2 \operatorname{Re}(A_0^{(0)*} A_0^{(6)}) \right. \\ \left. + \sum_{k=-2}^2 2 \operatorname{Re}(A_k^{(2)*} A_k^{(4)}) + O(E^8) \right). \quad (8)$$

The amplitudes $A_k^{(n)}$ can now be calculated from TDPT, which we use in the following form. For a Hamiltonian $\mathcal{H} = \mathcal{H}_0 + V(t)$, \mathcal{H}_0 having eigenstates $|A\rangle, |B\rangle, \dots$ with energies E_A, E_B, \dots and for $V(t)$ vanishing outside of $0 < t < T$, the evolution operator $U(T, 0)$ has matrix elements¹¹

$$\langle A | U(T, 0) | B \rangle = \langle A | B \rangle e^{-iE_A T} + (i\hbar)^{-1} \int_0^T dt e^{-iE_A(T-t)} \langle A | V(t) | B \rangle e^{-iE_B(t-0)} \\ + (i\hbar)^{-2} \int_0^T dt_2 \int_0^{t_2} dt_1 \sum_N e^{-iE_A(T-t_2)} \langle A | V(t_2) | N \rangle e^{-iE_N(t_2-t_1)} \langle N | V(t_1) | B \rangle e^{-iE_B(t_1-0)} + O(V^3). \quad (9)$$

In our application the initial and final states A and B are both S ; the sums over complete sets of states include only S , P , P' , D , and D' ; and the operator $V(t)$ is

$$V(t) = -eEz \sin(\pi t/T) \cos(\omega t + \delta). \quad (10)$$

Expanding the cosine in exponentials, and then putting $V(t)$ into the above expansion, one can easily separate the complete amplitude A into components of order E^n and $e^{ik\delta}$; i.e., the terms $A_k^{(n)}$. The leading term $A_0^{(0)}$ of the TDPT expansion is just $\langle S|S\rangle e^{-iE_S T} = e^{-iE_S T}$. This term describes the unperturbed evolution of the S state for time T . All terms $A_k^{(n)}$ with n or k odd vanish be-

cause of the dipole selection rules.

To obtain the signal to order E^2 we require the amplitude $A_0^{(2)}$, which upon expansion becomes the sum of four terms, which may be represented as

$$\begin{aligned} & S(+\omega)P(-\omega)S, \quad S(-\omega)P(+\omega)S, \\ & S(+\omega)P'(-\omega)S, \quad S(-\omega)P'(+\omega)S, \end{aligned} \quad (11)$$

where the capital letters denote the "path" of states by which the transition occurs (in Feynman's sense), time increases to the left, and the $(+\omega)$ and $(-\omega)$ denote the use of the positive or negative frequency parts of the cosine in $V(t)$. More explicitly, the first of these terms, as shown in Fig. 3, is

$$\begin{aligned} & (i\hbar)^{-2} \int_0^T dt_2 \int_0^{t_2} dt_1 e^{-iE_S(T-t_2)} \langle S|-eEz/2|P\rangle \sin(\pi t_2/T) e^{+i\omega t_2} \\ & \quad \times e^{-iE_P(t_2-t_1)} \langle P|-eEz/2|S\rangle \sin(\pi t_1/T) e^{-i\omega t_1} e^{-iE_S(t_1-0)} \\ & = \left(\frac{eE}{2i\hbar}\right)^2 \langle S|z|P\rangle \langle P|z|S\rangle e^{-iE_S T} \int_0^T dt_2 \int_0^{t_2} dt_1 \sin(\pi t_2/T) \sin(\pi t_1/T) e^{it_2(E_S+\omega-E_P)} e^{it_1(E_P-\omega-E_S)}. \end{aligned} \quad (12)$$

It is clear that for $E_S + \omega - E_P = 0$, or more precisely, for $\omega = \text{Re}(E_P - E_S)$, this integral "resonates," and in fact describes the ordinary one-photon S - P transition used in Lamb-shift measurements. In our application, however, $\omega/2\pi \approx 2025$ MHz, while $\text{Re}(E_P - E_S)/2\pi \approx 2970$ MHz, so this term is far from resonant. If we denote the above integral by $J(\omega, P)$, then we have

$$A_0^{(2)} = J(\omega, P) + J(-\omega, P) + J(\omega, P') + J(-\omega, P'). \quad (13)$$

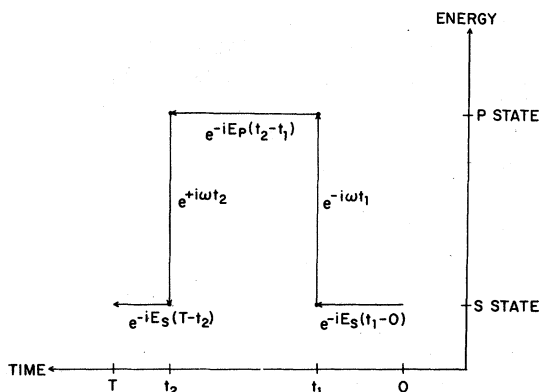


FIG. 3. Graphical representation of the "path" $S(+\omega)P(-\omega)S$ in the amplitude $A_0^{(2)}$.

The same integral serves in the computation of the amplitudes $A_{\pm 2}^{(2)}$, which are needed in calculating the signal to order E^4 . $A_{\pm 2}^{(2)}$ can be represented as the sum of two terms,

$$S(\pm\omega)P(\pm\omega)S \text{ and } S(\pm\omega)P'(\pm\omega)S. \quad (14)$$

Both terms are insignificantly small, since they are "energy-nonconserving" transitions, allowed only by the finite interaction time. Since they are on the order of 10^{-6} relative to the energy-conserving amplitudes, these terms can be safely dropped.

The other amplitude needed to complete the calculation of the signal to order E^4 is $A_0^{(4)}$. It is the sum of many "paths," the most important of which is

$$S(+\omega)P(+\omega)D(-\omega)P(-\omega)S. \quad (15)$$

This term may be thought of as describing a transition from S to D via the intermediate state P , and then a transition from D back to S via the same intermediate state. The term is resonant for $2\omega = \text{Re}(E_D - E_S)$, even though the intermediate S - P and P - D transitions are far from resonant. Again the quadruple integral can be evaluated analytically; the same general fourfold integral serves to calculate all 53 other terms of $A_0^{(4)}$, of which the most important are those such as

$S(+\omega)P(-\omega)S(+\omega)P(-\omega)S$, i.e., having sequence $SXSYS$, where X and Y are P or P' .

Included among the many paths are those with state sequence $SXD'YS$, which mark the first appearance of the D' state into the problem. Such terms describe two photon $S-D'$ transitions, which resonate at $\omega/2\pi \approx 1500$ MHz. With the typical experimental linewidths of $10 \sim 15$ MHz (in $\omega/2\pi$), this transition is well resolved from the $S-D$ resonance of interest at $\omega/2\pi \approx 2025$ MHz, and the effects of its overlap are negligible. Further consideration of the effects of the D' state is left to Sec. IX.

This suffices to give an expression for the signal complete through order E^4 , from which the line shape and line centers can be calculated, although the form of the analytical results is sufficiently

complicated that a computer evaluation is required. Before discussing any of the results, we introduce an approximation technique by which all these results can be obtained with negligible error, with much less effort, and with more physical insight.

V. EFFECTIVE POTENTIAL APPROXIMATION

The basic idea of the "effective potential" approximation is to describe two-step processes such as S to P to D as a single step process, S to D , with an effective potential. To derive the form of the effective potential, we consider the amplitude of order E^2 and $e^{-2i\theta}$ for a transition by time t from S to D , which has the form

$$\begin{aligned} (i\hbar)^{-2} \int_0^t dt_2 \int_0^{t_2} dt_1 e^{-iE_D(t-t_2)} \langle D | -eEz/2 | P \rangle \sin(\pi t_2/T) \\ \times e^{-i\omega t_2} e^{-iE_P(t_2-t_1)} \langle P | -eEz/2 | S \rangle e^{-i\omega t_1} \sin(\pi t_1/T) e^{-iE_S(t_1-0)} \\ = \left(\frac{eE}{2i\hbar} \right)^2 \langle D | z | P \rangle \langle P | z | S \rangle e^{-iE_D t} \int_0^t dt_2 \int_0^{t_2} dt_1 \sin(\pi t_2/T) \sin(\pi t_1/T) e^{it_2(E_D - \omega - E_P)} e^{it_1(E_P - \omega - E_S)}. \end{aligned} \quad (16)$$

We change to new integration variables $\sigma = \frac{1}{2}(t_2 + t_1)$, $\tau = t_2 - t_1$ so that τ represents the time spent in the intermediate P state. The region of integration is that labeled A in Fig. 4. We now make the approximation of adding the region labeled B to the integration region; that is, we extend the upper limit of the τ integration from the boundary of region A to $\tau = \infty$. The error incurred by doing

so should be small for two reasons. First, the integrand is exponentially damped in the large τ region by the decay rate of the intermediate P state; second, the integrand is rapidly oscillating in τ because of the large "energy defect" of the intermediate state. The integral now takes the form

$$(eE/2i\hbar)^2 \langle D | z | P \rangle \langle P | z | S \rangle e^{-iE_D t} \int_0^t d\sigma e^{i\sigma\beta} \int_0^\infty d\tau e^{i\tau\alpha} \frac{1}{2} [\cos(\pi\sigma/T) - \cos(2\pi\tau/T)], \quad (17)$$

where $\alpha = \frac{1}{2}(E_S + E_D) - E_P$ measures the energy defect of the intermediate state, and $\beta = E_D - 2\omega - E_S$ measures the detuning from the two-photon resonance. The substitution of $\tau = \infty$ as the upper limit of the inner integral now allows the integral

to be performed trivially, and one finds that the amplitude is given by

$$(i\hbar)^{-1} \int_0^t d\sigma e^{-iE_D(t-\sigma)} V_{\text{eff}}(\sigma) e^{-iE_S(\sigma-0)} \quad (18)$$

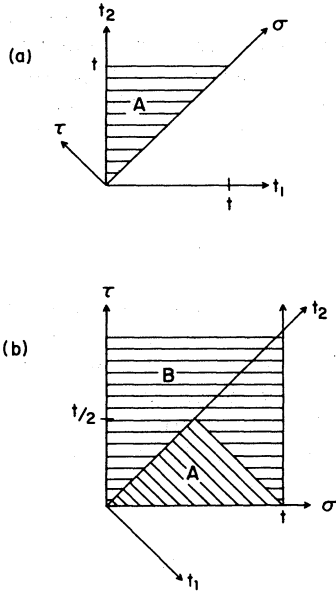


FIG. 4. $t_1 t_2$ plane for the integral in Eq. (16), showing the $\sigma\tau$ coordinate axes and the regions A and B of integration.

where

$$V_{\text{eff}}(\sigma) = (\hbar\alpha)^{-1} (eE/2)^2 \langle D|z|P\rangle \langle P|z|S\rangle e^{-2i\omega\sigma} \times \left[\sin^2(\pi\sigma/T) + \frac{1}{2} \frac{\pi^2/T^2}{\alpha^2 - \pi^2/T^2} \right]. \quad (19)$$

The important point is that the single integral which remains has exactly the form of a first-order TDPT amplitude for a transition from S to D , via the "effective potential" $V_{\text{eff}}(\sigma)$. One further approximation can be made for convenience; one finds, for values of α and T of interest, that the term added in brackets to $\sin^2(\pi\sigma/T)$ has

magnitude $\approx 18 \times 10^{-6}$, which is negligible compared to unity. We write the final form of the effective potential as

$$V_{\text{eff}}(D \leftarrow S)(t) = (\hbar\alpha)^{-1} (eE/2)^2 \langle D|z|P\rangle \langle P|z|S\rangle \times e^{-2i\omega t} \sin^2(\pi t/T). \quad (20)$$

Similarly the effective potential for the D to S transition is

$$V_{\text{eff}}(S \leftarrow D)(t) = (\hbar\alpha)^{-1} (eE/2)^2 \langle S|z|P\rangle \langle P|z|D\rangle \times e^{+2i\omega t} \sin^2(\pi t/T). \quad (21)$$

Just as these potentials are appropriate for the paths $D(-\omega)P(-\omega)S$ and $S(+\omega)P(+\omega)D$, respectively, we can by the same procedure find an effective potential corresponding to the sum of the four paths $S(\pm\omega)P(\mp\omega)S$ and $S(\pm\omega)P'(\mp\omega)S$:

$$V_{\text{eff}}(S \leftarrow S)(t) = \sum_{N=P, P'; a=\pm\omega} (\hbar\delta)^{-1} (eE/2)^2 \langle S|z|N\rangle \times \langle N|z|S\rangle \sin^2(\pi t/T), \quad (22)$$

where $\delta = E_S + a - E_N$, and for the sum of the two paths $D(\pm\omega)P(\mp\omega)D$

$$V_{\text{eff}}(D \leftarrow D)(t) = \sum_{a=\pm\omega} (\hbar\epsilon)^{-1} (eE/2)^2 \langle D|z|P\rangle \times \langle P|z|D\rangle \sin^2(\pi t/T), \quad (23)$$

where $\epsilon = E_D + a - E_P$.

The utility of these approximate results remains to be tested. To do so we write the approximate results

$$A_0^{(2)} = (i\hbar)^{-1} \int_0^T dt e^{-iE_S(T-t)} V_{\text{eff}}(S \leftarrow S)(t) e^{-iE_S(t-0)}; \quad (24a)$$

$$A_0^{(4)} = (i\hbar)^{-2} \int_0^T dt_2 \int_0^{t_2} dt_1 e^{-iE_S(T-t_2)} V_{\text{eff}}(S \leftarrow D)(t_2) e^{-iE_D(t_2-t_1)} V_{\text{eff}}(D \leftarrow S)(t_1) e^{-iE_S(t_1-0)} + (i\hbar)^{-2} \int_0^T dt_2 \int_0^{t_2} dt_1 e^{-iE_S(T-t_2)} V_{\text{eff}}(S \leftarrow S)(t_2) e^{-iE_S(t_2-t_1)} V_{\text{eff}}(S \leftarrow S)(t_1) e^{-iE_S(t_1-0)}; \quad (24b)$$

and evaluate these integrals analytically as before. Using these approximate amplitudes in place of the exact TDPT ones calculated earlier we can again evaluate the signal defined by Eq.

(8). This procedure gives a second way of calculating the signal complete through order E^4 , but with the advantages that the dimensionality of the integrals required is reduced from 4 to 2, and

that fewer terms need to be considered.

Results for the signal in order E^4 are shown in Fig. 5. (Not included is the nonresonant background of order E^2 and E^4 , which may be thought of as the far wing of the S - P resonance at 2970 MHz.) A discussion of the detailed form of the two-photon resonance is postponed to Sec. VI; of immediate interest is the difference between the "exact" and "effective potential" TDPT results. The magnitude of the difference is $< 10^{-3}$ of the signal; variations in the difference with frequency are $\lesssim 10^{-4}$ of the signal; the symmetry of the difference about the line center is high enough that symmetric point line centers calculated from the two different expressions agree everywhere to $\lesssim 0.3$ kHz, where the linewidth is ≈ 12 MHz and the center frequency 2025 MHz.

This very impressive agreement vindicates *a posteriori* the approximations made in deriving the effective potentials, and strongly stimulates their further use in applications to follow. In summary, even in a high-precision experiment, where a description of a line shape to $\lesssim 10^{-3}$ of its width is crucial, the effective potential gives a very accurate description of the dynamics of the two-photon transition process.

A very useful property of this method is that it is not limited to monochromatic excitations, but accommodates the envelope function $\sin(\pi t/T)$. The derivation can be repeated for a Gaussian envelope $\exp(-t^2/T^2)$, and results in an effective potential with the factor $\exp(-2t^2/T^2)$. Any general envelope function $f(t)$ will give an effective potential with $f^2(t)$, subject to the qualification that small correction terms of order $(\alpha T)^{-2}$ will appear, where T measures the scale of time variation of the envelope function. [The term of order $(\alpha T)^{-2}$ we dropped above was just such a term.] Physically, this requires that the product of the energy defect and the transit time be large compared to Planck's constant. In our application $\alpha = \frac{1}{2}(E_S + E_D) - E_P$ and $\text{Re}(\alpha)/\hbar \sim 1$ GHz, or $\text{Re}(\alpha) \sim 6 \times 10^9$ sec $^{-1}$ in units where $\hbar = 1$. With characteristic T 's on the order of 80 nsec, we have $\alpha T = 480$, which is satisfactorily large, since it will enter only as an inverse square. In most optical experiments the energy defect will be of optical, rather than

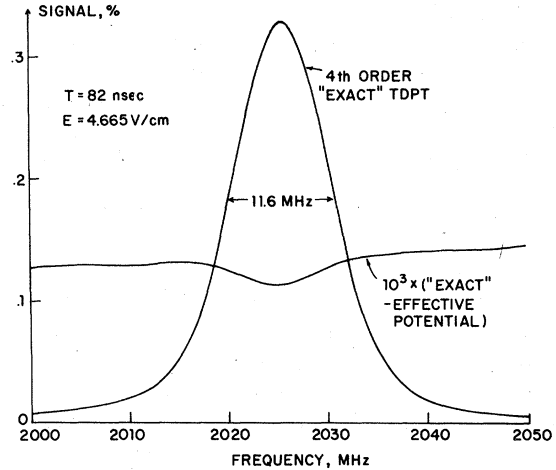


FIG. 5. Two-photon resonance signal to order E^4 , showing the "exact" result [Eq. (15)], and 10^3 times the difference between this and the "effective potential" result [Eq. (24)], evaluated for $T = 82$ nsec.

microwave, scale; and T will be larger for thermal than for fast beams. Thus the effective potential technique should be just as useful in laser studies as it is here.

The main limitation of this technique is that it requires a sufficiently large energy defect; as a result it is not applicable to situations with a near-resonant intermediate state.

VI. TWO-PHOTON LINE SHAPE AND THE LIFETIME SHIFT

We now consider in detail the line shape predicted in the effective potential approximation, since it agrees with the corresponding "exact" TDPT result to high accuracy.

The signal Eq. (8) to order E^2 requires only $A_0^{(0)} = e^{-iE_S T}$ and $A_0^{(2)}$ of Eq. (24a), which is

$$A_0^{(2)} = -ie^{-iE_S T} \sum_{N=P, P'; a=\pm\omega} (eE/2\hbar)^2 \delta^{-1} \langle S|z|N \rangle \times \langle N|z|S \rangle (T/2). \quad (25)$$

To order E^2 the signal is

$$S(\omega, E) = -|A_0^{(0)}|^2 2\text{Re}(A_0^{(0)*} A_0^{(2)}) = (eE/2\hbar)^2 (T/2) \sum_{N=P, P'; a=\pm\omega} \langle S|z|N \rangle^2 \frac{\Gamma_N - \Gamma_S}{(\omega_S + a - \omega_N)^2 + (\Gamma_S - \Gamma_N)^2/4}. \quad (26)$$

This form of the signal shows a superposition of four Lorentzian resonances centered at $\omega = \pm|\omega_S - \omega_N|$. For the problem at hand, ω is near

none of these resonances, so the signal in this order is a nearly constant background. This represents the quenching of the S state by an admixture of the

shorter-lived P and P' states. Because ω is far from any one of these single-photon resonances, both the "rotating" and "counter-rotating" terms of the field contribute importantly to the signal.

To compute the signal to order E^4 we require $A_0^{(4)}$, which from Eq. (24b) is seen to be the sum of two paths which may be represented as $S(+2\omega)D(-2\omega)S$ and $S(+0\omega)S(+0\omega)S$. The latter term, together with $|A_0^{(2)}|^2$ in Eq. (8), represent a higher order of nonresonant S state quenching due to P and P' admixture, and slightly modifies the sloping background that underlies the two-photon resonance. Guided by earlier results, we now drop the "energy-nonconserving" terms $|A_{\pm 2}^{(2)}|^2$.

The first line of $A_0^{(4)}$ of Eq. (24b), representing the two-photon $S - D$ transition of interest, requires only a double integration, and has the value

$$A_0^{(4)}(S - D) = -(eE/2\hbar)^4 |\langle S|z|P\rangle|^2 \times |\langle P|z|D\rangle|^2 \alpha^{-2} e^{-iE_S T} K(\beta), \quad (27)$$

where

$$K(\beta) = [16\beta(\beta^2 - 4\pi^2/T^2)]^{-1} \times [8i(2\pi/T)^4 e^{i\beta T/2} \sin(\beta T/2) \times \beta^{-1}(\beta^2 - 4\pi^2/T^2)^{-1} - 2iT(3\beta^2 - 2(2\pi/T)^2)]. \quad (28)$$

The meaning of this result can be seen much more clearly if we treat α and β as real numbers, i.e., we temporarily neglect the lifetimes of the S , P , and D states. Then the resonant part of the fourth-order signal is

$$S(\omega, E) = (eE/2\hbar)^4 |\langle S|z|P\rangle|^2 |\langle P|z|D\rangle|^2 \times \alpha^{-2} (2\pi/T)^4 \times \frac{1}{2} [\sin(\beta T/2) \beta^{-1} (\beta^2 - 4\pi^2/T^2)^{-1}]^2, \quad (29)$$

where the two-photon line shape is given by the last factor in this expression. It describes a resonant shape peaked at $\beta = E_D - 2\omega - E_S$ which has its first zeros at $\beta = \pm 4\pi/T$ or at $\nu = \frac{1}{2}(\nu_D - \nu_S) \pm 1/T$. This predicts a full width at zero height of $2/T$, or a FWHM of the order of $1/T$ (in the ν energy scale, where $\nu = \omega/2\pi \approx 2025$ MHz is the location of the resonance). Since T is about 80 nsec, we expect 12 MHz or so of the experimental linewidths to result from the transit time and the field envelope. Actually the parameter β is complex, and this effect, representing the decay of

the states involved, will further broaden the resonance.

The other point of interest is that the resonance line is symmetric, since it is an even function of β . We can easily show that this symmetry persists for complex β , provided α is real. Since $\beta = (\omega_D - 2\omega - \omega_S) - \frac{1}{2}i(\Gamma_D - \Gamma_S)$, $-\beta^* = -(\omega_D - 2\omega - \omega_S) - \frac{1}{2}i(\Gamma_D - \Gamma_S)$, so the replacement $\beta \rightarrow -\beta^*$ is equivalent to moving from one side of the resonance's center $\omega = \frac{1}{2}(\omega_D - \omega_S)$ to the symmetric point on the other side. Under the replacement $\beta \rightarrow -\beta^*$, $K(\beta) \rightarrow K(-\beta^*)$, and by explicit computation one finds $K(-\beta^*) = K(\beta)^*$. Since for α real the signal depends only on $\text{Re} K(\beta)$, we see that the signal is unchanged under $\beta \rightarrow -\beta^*$ and hence is symmetric about $\omega = \frac{1}{2}(\omega_D - \omega_S)$.

This symmetry disappears, however, when α is complex. Since

$$\alpha = \frac{1}{2}(E_S + E_D) - E_P = \frac{1}{2}(\omega_S + \omega_D - 2\omega_P) - \frac{1}{4}i(\Gamma_S + \Gamma_D - 2\Gamma_P), \quad (30)$$

it is convenient to define $\alpha = -\alpha_0 e^{-i\phi}$, where α_0 and ϕ are real and positive, and where $\phi \approx 6.5$ mrad. With $\phi \ll 1$, we can write

$$\text{Re}[\alpha^{-2} K(\beta)] \approx \alpha_0^{-2} [\text{Re} K(\beta) - 2\phi \text{Im} K(\beta)]. \quad (31)$$

Since under $\beta \rightarrow -\beta^*$, $K(\beta) \rightarrow K(\beta)^*$ we see that $\text{Im} K(\beta) \rightarrow -\text{Im} K(\beta)$; hence the coefficient of 2ϕ in Eq. (31) changes sign upon moving from one side of the resonance to the other, showing that the line is not symmetric about the assumed center $\omega = \frac{1}{2}(\omega_D - \omega_S)$. In fact, $\text{Im} K(\beta)$ has a dispersive shape about resonance, and has a magnitude comparable to $\text{Re} K(\beta)$, so that the effect of the term in 2ϕ in Eq. (31) is to shift the center of the resonance by about $2\phi \approx 1.3\%$ of its width. Some asymmetry about the new shifted center is also introduced, since $\text{Im} K(\beta)$ differs from the derivative with respect to β of $\text{Re} K(\beta)$.

Let us step back a moment from the details of the computation and briefly summarize the implications of this result. We have found that the S to S transmission probability shows an $S - D$ two-photon resonance centered not at the expected Bohr frequency $\omega = \frac{1}{2}(\omega_D - \omega_S)$, but shifted from it by a fraction of the resonance's linewidth. Since this effect appears in the same order of TDPT as does the two-photon resonance, it does not disappear at low power levels; it is intrinsic to the transition process. We choose to call this novel effect the "lifetime shift," since it is of magnitude $2\phi \times \text{linewidth}$, where ϕ is the lifetime related phase of the energy defect. This energy defect makes its appearance as an energy denom-

inator in both effective potentials $V_{\text{eff}}(S \rightarrow D)$ and $V_{\text{eff}}(D \rightarrow S)$ (though we must emphasize that the lifetime shift is not an artifact of the effective potential approximation, since it is reproduced both in the "exact" TDPT computation and in a calculation of Shirley's type).¹⁵ The fourth-order S to S amplitude, containing the product of these effective potentials, thus contains a phase of 2ϕ . Because the fourth-order signal arises from the interference of this and the zero-order S to S amplitude, the phase is physically observable.

It follows that the S to D transition probability, which is proportional to the absolute square of $V_{\text{eff}}(D \rightarrow S)$, will show no lifetime shift, since $|e^{-i\phi}|^2 = 1$. Thus the signal corresponding to the creation of D states will (in fourth order) be centered at the expected Bohr frequency. There is no paradox in having the S to S and S to D signals centered at different frequencies, since the usual unitarity arguments to the contrary fail to apply, given a non-Hermitian Hamiltonian.

These observations also suggest that the lifetime shift will rarely be important in optical two-photon transitions. Such transitions are usually observed by monitoring the upper-state fluorescence, where the argument of the previous paragraph shows that the shift will be absent. Furthermore, we can see that the phase ϕ will be proportional to the quotient of the "decay rate defect" and the "energy defect," i.e., $\phi \propto (\Gamma_S + \Gamma_D - 2\Gamma_P)/(\omega_S + \omega_D - 2\omega_P)$. In the optical case, the energy defects are in general very much larger, while the decay rate defects are about the same size as those encountered here. Therefore, it is not surprising that the effects of the lifetime shift have not been observed in the optical regime.

VII. POWER SHIFT

Having completed the calculation of the signal [Eq. (5)] to the lowest order in which the two-photon resonance appears, we now treat the next order in E , which yields the linear power shift of the resonance. Referring to Eq. (8), we need the S to S amplitude $A_0^{(6)}$. The other sixth-order term in Eq. (8), which depends on $\sum_{k=-2}^2 A_k^{(2)*} A_k^{(4)}$, can be approximated by $A_0^{(2)*} A_0^{(4)}$, since we drop the "energy-nonconserving" parts; thus this term requires no new computation.

The new amplitude $A_0^{(6)}$ we calculate only in the effective potential approximation, our confidence bolstered by the success of this technique in second and fourth order. The amplitude can be represented as the sum of four paths,

$$\begin{aligned} & S(+0\omega)S(+0\omega)S(+0\omega)S, \quad S(+0\omega)S(+2\omega)D(-2\omega)S, \\ & S(+2\omega)D(+0\omega)D(-2\omega)S, \quad S(+2\omega)D(-2\omega)S(+0\omega)S. \end{aligned} \quad (32)$$

The first of these does not involve the D state, and is another contribution to the nonresonant background, similar to the second- and fourth-order contributions. The remaining three paths represent S to D to S transitions, with the S or D state affected by coupling to the P or P' state. One may think of these as rf Stark shifts of the S and D states. The last path, more explicitly, contributes to $A_0^{(6)}$ the term

$$\begin{aligned} (i\hbar)^{-3} \int_0^T dt_3 \int_0^{t_3} dt_2 \int_0^{t_2} dt_1 e^{-iE_S(T-t_3)} \\ \times V_{\text{eff}}(S \rightarrow D)(t_3) e^{-iE_D(t_3-t_2)} \\ \times V_{\text{eff}}(D \rightarrow S)(t_2) e^{-iE_S(t_2-t_1)} \\ \times V_{\text{eff}}(S \rightarrow S)(t_1) e^{-iE_S(t_1-0)}. \end{aligned} \quad (33)$$

Calculating the signal through sixth order, one finds that the center of the resonance moves to higher frequency with increasing electric field strength. In Sec. VIII we discuss in more detail the size of this power shift. The magnitude of the linear power shift can be derived from the behavior of the line center in the region of small E , where TDPT is certainly a good approximation, and the shift rates thus obtained are firmly tied to first principles, including in their computation the effects of both the envelope function of the microwave field and the decay rates of the states involved.

One discouraging result is that for values of E used in the experiment $E = 15 \sim 25$ V/cm, the sixth-order contributions to the signal dominate the fourth-order terms, suggesting that even higher-order terms are important in this regime.

VIII. EFFECTIVE POTENTIAL TWO-LEVEL PROBLEM

The behavior of the sixth-order terms in the signal for values of E of experimental interest motivates us to consider yet higher-order terms in the TDPT expansion. In addition to yielding the quadratic and higher-order power shifts of the resonance, such studies can be used to find the saturation behavior of the two-photon resonance, i.e., how its size grows with increasing E . Since the depletion of the S states in the interaction region can be no more than 100%, it is clear that the signal defined by Eq. (5) cannot exceed 1 for any value of E . But any finite order of perturbation theory, truncated at order E^n , will eventually show the signal growing as E^n , which will exceed 1 for some value of E .

These considerations motivate a nonperturbative treatment of the problem. A direct numerical solution of the multilevel Schrödinger equation is possible in principle, but infeasible in practice, since the physical importance of rapidly oscillating, nonresonant terms cannot be neglected. We have instead developed a nonperturbative use of the effective potential approximation which avoids these numerical problems and provides a very economical solution to the problem.

The point of departure for this solution is the observation that the TDPT expansion using the effective potentials of Secs. V–VII is a perturbative treatment of a two-level problem specified by an “effective Hamiltonian”

$$\mathcal{H}_{\text{eff}} = \begin{bmatrix} E_S & 0 \\ 0 & E_D \end{bmatrix} + \begin{bmatrix} V_{\text{eff}}(S \leftarrow S)(t) & V_{\text{eff}}(S \leftarrow D)(t) \\ V_{\text{eff}}(D \leftarrow S)(t) & V_{\text{eff}}(D \leftarrow D)(t) \end{bmatrix}. \quad (34)$$

More specifically, the perturbative treatment of this \mathcal{H}_{eff} will result in exactly the expansion already made (through order E^6) in the effective potential approach. The new idea of this section is to use this Hamiltonian nonperturbatively.

This approach cannot claim to be an exact solution of the original problem, since the effective potentials themselves were derived from perturbation theory. In particular, the P and P' states are not dynamically included in the two-level problem specified above. Nevertheless, their influence is incorporated in the form of the effective potentials.

An appropriate transformation can be applied to the above Hamiltonian to remove the time dependence of its off-diagonal elements, without any effect on the S to S transition amplitude of interest. The transformed Hamiltonian is

$$\mathcal{H}'_{\text{eff}} = \begin{bmatrix} E_S + \omega & 0 \\ 0 & E_D - \omega \end{bmatrix} + \left(\frac{eE}{2\hbar}\right)^2 \sin^2\left(\frac{\pi t}{T}\right) \begin{bmatrix} \sum_{N,a} \delta^{-1} |\langle S|z|N \rangle|^2 & \alpha^{-1} \langle S|z|P \rangle \langle P|z|D \rangle \\ \alpha^{-1} \langle D|z|P \rangle \langle P|z|S \rangle & \sum_a \epsilon^{-1} |\langle D|z|P \rangle|^2 \end{bmatrix}. \quad (35a)$$

The remarkable thing about this Hamiltonian is that it has the form

$$\mathcal{H}'_{\text{eff}} = C + W \sin^2(\pi t/T), \quad (35b)$$

where C and W are constant complex matrices, and C is diagonal. The only time dependence is $\sin^2(\pi t/T)$, which is very “slow,” going through only one cycle during the interaction time. The result is a system which can be integrated numerically with no computational difficulties and no great numerical effort. The quantity of interest is the complex 2×2 evolution operator $U(t)$ which satisfies the conditions $U(0) = 1$, $i dU/dt = \mathcal{H}'_{\text{eff}} U(t)$. The S -state transmission probability is given by $|U(T)_{11}|^2$, and the experimental signal defined by Eq. (5) can be calculated as before.

The results agree, in the appropriate regime, with the results of the effective potential TDPT discussed above, which in turn agree, where appropriate, with the original first-principles TDPT expansion. The agreement is perfect, in the sense that line centers obtained by the TDPT and nonperturbative methods agree to better than 1 kHz, and power shift rates agree to three digits or better. This provides a valuable procedural test, since the computational tasks are very much

different for the two theoretical approaches. The numerical integration of a matrix differential equation is needed for the matrix treatment, and the numerical evaluation of analytically computed integrals is used for the TDPT method. The matrix approach differs from the TDPT results in the large- E region, where it provides (in some sense) a nonperturbative solution.

The form of the above two-level Hamiltonian can also be used to shed some physical insight on the power shift. For our present purposes we can neglect the lifetime shift, which is due to the phase of the off-diagonal elements of $\mathcal{H}'_{\text{eff}}$, and for conceptual simplicity we can imagine that the magnitude of these elements is very small. Then to lowest order, the two-photon resonance occurs at the crossing of the diagonal elements of C , i.e., when $\text{Re}[(E_D - \omega) - (E_S + \omega)] = 0$, which gives as line center the Bohr condition $2\omega = \omega_D - \omega_S$. The power shift first appears when the effects of the on-diagonal terms of W are considered. At the center of the interaction region these terms have the effect of shifting the S - and D -state energies according to

$$E_S \rightarrow E_S + (eE/2\hbar)^2 \Lambda_S, \quad (36a)$$

$$\Lambda_S = \sum_{N=P, P'; a=\pm\omega} (E_S + a - E_N)^{-1} | \langle S | z | N \rangle |^2, \quad (36b)$$

$$E_D \rightarrow E_D + (eE/2\hbar)^2 \Lambda_D, \quad (36c)$$

$$\Lambda_D = \sum_{a=\pm\omega} (E_D + a - E_P)^{-1} | \langle D | z | P \rangle |^2. \quad (36d)$$

To incorporate the effects of the shape of the field envelope, we can take a simple time average of the local shift, averaged over the total interaction time. This produces an average shift of $\frac{1}{2}$ the size of that obtained at the center of the interaction region, so that the resonance condition is

$$\begin{aligned} \text{Re}[(E_D - \omega + \frac{1}{2}(eE/2\hbar)^2 \Lambda_D) \\ - (E_S + \omega + \frac{1}{2}(eE/2\hbar)^2 \Lambda_S)] = 0, \end{aligned} \quad (37)$$

or

$$2\omega = \omega_D - \omega_S + \frac{1}{2}(eE/2\hbar)^2 \text{Re}(\Lambda_D - \Lambda_S). \quad (38)$$

This predicts that the power shift is quadratic in E , i.e., linear in power, that it is independent of the interaction time T , and that it has $\frac{1}{2}$ the steady-state value that would apply for an atom at rest in the center of the interaction region. One can also perform a somewhat more sophisticated time average by weighting the size of the local shift in each part of the interaction region by the local probability for inducing a two-photon transition, which probability also has the shape of the square of the field envelope. Such an average, performed for the $\sin^2(\pi t/T)$ envelope appropriate for the Hamiltonian above, changes the power shift from $\frac{1}{2}$ to $\frac{3}{4}$ of the steady-state or peak value. This result is within a few percent of the values obtained by the more involved methods described above. Similarly, for a field with Gaussian envelope, this sort of transition probability weighted average yields a net power shift of $2^{-1/2}$ of the peak shift appropriate to the center of the interaction region.

Naturally, the above calculations are no substitute for obtaining the actual power-shifted line shape, but they do serve to illuminate the physical processes that occur.

IX. REFINEMENTS OF THE LINE SHAPE CALCULATION

We return now to some effects postponed in the earlier analysis of the two-photon line shape, in the process demonstrating the flexibility of the TDPT and effective potential approximations.

We first consider further effects of the D' state than the negligible ones discussed in Sec. IV. In higher orders of TDPT, the presence of the D' state makes possible many new "paths" which have the physical effect of modifying the power shift of the S - D resonance. To investigate these

effects, we have generalized the effective potential matrix approach to a 3×3 matrix in which S , D , and D' states are treated on an equal footing. Results obtained from this analysis show changes in the size of the power shift of the S - D resonance well below the 0.1% level.

An important class of effects arises from a more complete description of the microwave electromagnetic field than Eq. (1) provides. If we set up a coordinate system in the waveguide with the atoms moving in the \hat{y} direction, the microwaves propagating along the \hat{x} axis, and with the electric field still having a z polarization, then the electromagnetic fields appropriate to the propagating TE_{10} mode are given by the real parts of¹⁶

$$E_x = E \sin(\pi y/a) \exp(ikx - i\omega t), \quad (39a)$$

$$B_x = -(kc/\omega)E \sin(\pi y/a) \exp(ikx - i\omega t), \quad (39b)$$

$$B_z = (\pi c/i\omega a)E \cos(\pi y/a) \exp(ikx - i\omega t), \quad (39c)$$

where a is the width of the waveguide in the y direction, and k is given by

$$k = (\omega/c)[1 - (\pi c/\omega a)^2]^{1/2}. \quad (40)$$

The most important new effects arise from a Lorentz transformation to the atoms' rest frame, which has lab velocity $\vec{v} = v\hat{y}$, according to the usual formulas

$$t' = t(1 - v^2/c^2)^{-1/2}, \quad (41a)$$

$$E'_x = (1 - v^2/c^2)^{-1/2}(E_x - vB_x/c). \quad (41b)$$

The first transformation represents time dilation, and expresses the ordinary second-order Doppler shift, for which the data have to be corrected. The second yields here a novel effect, peculiar to the presence of longitudinal field components in waveguides, but not restricted to multiple-quantum processes. To order v/c , the electric field replacing Eq. (1) is

$$\begin{aligned} E(t) = E[\sin(\pi t/T) \cos(\omega t + \delta) \\ + (2N)^{-1} \cos(\pi t/T) \sin(\omega t + \delta)], \end{aligned} \quad (42)$$

where $N = \omega a/2\pi v$ is simply the number of microwave cycles occurring during the transit time T .

The effect of this new term is to shift the location of the observed resonance, as can most easily be seen by writing the above as

$$\begin{aligned} E(t) = E\{ (1 - 1/2N) \sin(\pi t/T) \cos(\omega t + \delta) \\ + (1/2N) \sin[(\omega + \pi/T)t + \delta] \}. \end{aligned} \quad (43)$$

This shows an "upper sideband" of magnitude $1/2N$ separated from the fundamental by $\Delta\omega = \pi/T$, which is approximately the resonance linewidth.

The result is a shift of order $\text{FWHM}/2N$, and since the linewidth and $1/2N$ both scale as the speed v , this shift is proportional to v^2 .

The importance of this shift arises from the fact that it does not change sign under reversal of either the atomic beam or the microwave propagation direction. In this respect it differs from the ordinary first-order Doppler shift, which is easily shown to have magnitude

$$\Delta\omega = kv \sin\theta \quad (44)$$

for an alignment error θ from exact perpendicularity between the atomic beam and the direction of microwave propagation.

The size of the shift entailed by the modified electric field [Eq. (42)] can be calculated by substituting the new form of $E(t)$ into the integral [Eq. (15)] for $A_0^{(4)}$ of Sec. IV and isolating the term of order $1/N$. It proves to be dispersive in shape, shifting the resonance as expected. Alternatively, one may repeat the derivation of the effective potentials with the modified form of the electric field to find

$$\begin{aligned} V_{\text{eff}}(D \rightarrow S)(t) = & (\hbar\alpha)^{-1} (eE/2)^2 \langle D|z|P \rangle \\ & \times \langle P|z|S \rangle e^{-2i\omega t} \\ & \times [\sin^2(\pi t/T) \\ & + (i/2N) \sin(2\pi t/T) + O(N^{-2})] \quad (45) \end{aligned}$$

with $V_{\text{eff}}(S \rightarrow D)$ showing an $O(N^{-1})$ correction of opposite sign, and the $S \rightarrow S$ and $D \rightarrow D$ effective potentials showing no $O(N^{-1})$ correction, to a consistent approximation. With these results, the effective potential matrix approach confirms the size of the shift at low power, and also shows that the shift has negligible power dependence.

Another feature present in the real experiment and not considered heretofore in the theory is the presence of holes in the side walls of the waveguide provided for the atomic beam's passage. The holes used had radius $R = 0.40$ cm, compared with the waveguide sidewall height of $b = \frac{1}{2}a = 6.46$ cm. The modifications to the electric field in the region of the holes can be calculated using the theory of Bethe.¹⁷ His solution is applicable for $kR \ll 1$; in the experiment here $kR \approx 0.17$. We can also make the "near-field" approximation, which corresponds to neglecting retardation of the electric field, again because $kr \ll 1$ for distances r from the hole of interest to us. The result relevant here is not the detailed shape of the electric field modifications near the hole, but rather their size and scale. One finds that the electric field in the hole is of $O(ER/a)$, and that along the beam trajectory modifications to the no-hole solution fall off quadratically with distance

on a scale of size R . Furthermore, the modifications are identical at the beam's entrance and exit holes.

The result is a microwave field retaining its symmetry about $t = \frac{1}{2}T$, with minor modifications in the $t = 0$ and $t = T$ regions. The effective potentials then have modifications of order $(ER/a)^2$ over regions of scale R , compared to the previous result of order E^2 over scale a . The net factor of $(R/a)^3$ is about 4×10^{-5} , and since the symmetry of the field distribution about $t = \frac{1}{2}$ is preserved, the changes introduced into the line shape will be at worst modifications to the power shift and lifetime shift of this order. Consequently the effects of the holes are negligible.

In addition to the modifications of the electric field mentioned so far, there are present in the experiment microwave electric fields of polarizations in other directions than z . These have the potentially serious effect of inducing $\Delta m_F = \pm 1$ transitions and coupling the $3^2S_{1/2}(F=0)$ state of interest to the undesired $3^2S_{1/2}(F=1)$ states. Such stray polarizations can arise in two ways. For atoms moving through the holes in the waveguide's side walls, but off the axis of the holes, electric fields of various polarizations are present. These have the approximate size and scale discussed above, and again have negligible effect on the resonance's center, since the factor of $(R/a)^3 = 4 \times 10^{-5}$ derived above is to be applied to the maximum imaginable shift that could arise from this mechanism, namely, the $3^2S_{1/2}$ hyperfine splitting, itself only 1% of the $S-D$ interval. Similarly, stray polarizations present within the waveguide proper, which arise from Lorentz transforming the microwave magnetic fields, have negligible effects.

The microwave magnetic fields do not induce magnetic dipole transitions to any appreciable extent, since their frequency is far from resonance with the hyperfine intervals, and since magnetic dipole transitions require much larger field strengths than do electric dipole transitions. A more subtle effect is the rf Zeeman shift of second order in the microwave magnetic field, analogous to the rf Stark shift of second order in the microwave electric field; this, however, only introduces corrections of order 5×10^{-5} in the size of the power shift.

Finally one may consider the effects of dc electric and magnetic fields. The experiment is performed in a field-free region, with the earth's magnetic field canceled by three orthogonal Helmholtz coils, so that the dc magnetic and motional electric fields are very small. Other electric fields may arise from space-charge effects due to the unneutralized component of the atomic

beam, or charge accumulation on insulating films deposited on metal surfaces in the interaction region. One can easily compute the dc Stark shift of the two-photon resonance to be

$$\Delta\nu = 26 F^2 \text{ kHz cm}^2/\text{V}^2 \quad (46)$$

out of a frequency of $\nu \approx 2025$ MHz, for dc electric field F . For field strengths appropriate to the experiment, this produces at most a shift of 5 kHz.

There is a very subtle shift, peculiar to the two-photon process, that may also be considered in this connection. The $S-D$ transition of interest proceeds by way of the $3^2P_{3/2}(F=1)$ state, which is nearly degenerate with the $3^2D_{3/2}(F=2)$ state, the hyperfine structure of the two levels fortuitously bringing them to within 0.4 MHz of each other. An electric field will mix these two states, causing an unimportant shift of the P -state energy, as well as increasing the lifetime of the P state by admixing the longer-lived D' state. This will change the lifetime shift of the two-photon resonance, but the size of the shift is negligible for typical field strengths.

X. CONCLUSIONS

We have developed in this paper a theory for the line shape of two-photon transitions, of sufficient detail to be useful in splitting to a small fraction of its width a resonance obtained in a realistic experimental situation. We now briefly review some of the capabilities, predictions, and limitations of the theory.

The spectrum of states incorporated by the theory consists of an initial state (S), an intermediate state (P), and a final state (D), together with other states (P' and D') coupled to them. We have chosen to calculate the transmission amplitude for the S state, though nothing in the formalism prevents calculating the creation amplitude for the D state. One could also incorporate the presence of more than one intermediate state. Both the intermediate-state P , and the state P' coupled to S but not to D , have been shown to influence the power shift of the resonance. In short, the TDPT approach can readily incorporate a rich and complicated spectrum of states.

We have in the theory accounted for an actual time envelope of the external (microwave) field with which the transitions are driven. This profile is all important in determining the shape, and particularly the width, of the resonance obtained. While the profile used had a sinusoidal shape, nothing in the formalism prevents applica-

tion of the theory to a Gaussian or even a numerically tabulated function.

The fact that the atomic states involved here have natural decay rates has been shown to produce a very interesting "lifetime shift." In addition to causing this shift, the lifetimes influence materially the linewidth to be expected in cases where the transit time is long compared to the lifetimes.

The development of the effective potential approximation has greatly simplified the TDPT calculations required, and also made physically transparent the similarities of two- to one-photon transitions, while still preserving all the spectroscopic accuracy of the theory. The further use of the effective potential matrix approximation has in large measure circumvented the perturbative features of the original TDPT expansion and produces, for instance, a saturation curve which could not be obtained in any finite order of perturbation theory.

Finally, the theory is sufficiently flexible that the small corrections required by any real experimental situation can readily be included. For example, the effect of motional microwave electric fields has been calculated in detail.

There remain, of course, some limitations to the theory. One restriction, the use of a single transit time for all the atoms, can be easily circumvented; a thermal beam experiment would simply require an appropriate velocity average over the several transit times of individual atoms. A more serious limitation is that the theory was developed for "beam" type experiments, in which interrogation and detection of the atoms are resolved in space or time, and it is perhaps unsuited to "bottle" or steady-state situations in which the separation cannot be made.

We have incorporated only a single polarization of radiation in the theory, because we have been able to achieve this desirable condition experimentally. The addition of other space components of the external field would entail more complexity, but not a fundamental change in the theory. We have also assumed a monochromatic external field, i.e., with sidebands generated only by the field envelope and finite transit time, and have not considered a case of some interest in laser physics, in which the intrinsic laser linewidth can be a dominant factor in the experimental linewidth.

In the companion paper we compare with experiment the many predictions of this theory for the $3^2S_{1/2} - 3^2D_{5/2}$ two-photon transition in hydrogen, and use it to reduce the data obtained there and derive a value for this hydrogenic fine-structure interval.

ACKNOWLEDGMENTS

We wish especially to acknowledge helpful discussions with Professor S. R. Lundeen. This

work was supported by the NSF under Grant No. PHY76-14857. One of the authors (D.A.V.B) was supported by a Charles Bayne Aiken Graduate Fellowship (1977-78).

*Present address: Physics Dept., Brandeis University, Waltham, Mass. 02154.

- ¹C. W. Fabjan and F. M. Pipkin, Phys. Rev. A 6, 556 (1972).
- ²S. R. Lundeen and F. M. Pipkin, Phys. Rev. Lett. 34, 1368 (1975).
- ³D. A. Andrews and G. Newton, Phys. Rev. Lett. 37, 1254 (1976).
- ⁴P. B. Kramer, S. R. Lundeen, B. O. Clark, and F. M. Pipkin, Phys. Rev. Lett. 32, 635 (1974).
- ⁵J. H. Shirley, Phys. Rev. 138, B979 (1965).
- ⁶H. Salwen, Phys. Rev. 99, 1274 (1955).
- ⁷E. A. Power and S. Zienau, Philos. Trans. R. Soc. London Ser. A 251, 427 (1959).
- ⁸E. A. Power and T. Thirunamachandran, Am. J. Phys. 46, 370 (1978).
- ⁹M. P. Silverman, Ph.D. thesis (Harvard University, 1973) (unpublished).
- ¹⁰G. W. Erickson (private communication).
- ¹¹S. J. Brodsky and R. G. Parsons, Phys. Rev. 163, 134 (1967).
- ¹²G. Breit, Phys. Rev. 35, 1447 (1930).
- ¹³P. Pyykkö and E. Pajanne, Phys. Lett. A 35, 53 (1971); and erratum, Phys. Lett. A 38, 218 (1972).
- ¹⁴M. T. Grisaru, H. N. Pendleton, and R. Petraso, Ann. Phys. 79, 518 (1973).
- ¹⁵B. O. Clark, Ph.D. thesis (Harvard University, 1976) (unpublished).
- ¹⁶J. D. Jackson, in *Classical Electrodynamics* (Wiley, New York, 1962), Chap. 8.
- ¹⁷H. A. Bethe, Phys. Rev. 66, 163 (1944).